on site and transported to Vancouver over dry ice. Voucher samples of each invertebrate were stored in methanol at −20°C at the University of British Columbia for taxonomic identification. Marine microorganisms were isolated from the invertebrates on site using various marine culture media, and pure cultures were grown as lawns on solid agar marine media in 10-cm Petri plates for several days and then freeze-dried. Extracts were prepared by homogenizing ~200 g of each invertebrate sample or entire microorganism cultures (cells and agar medium) in methanol. The homogenates were filtered and concentrated to dryness *in vacuo* to give a gummy residue. A small amount of each extract was dissolved in DMSO for the G_2 checkpoint inhibition assay.

Bioassay-guided Fractionation. Bacterial extract Clin-1116 was fractionated as follows: dried methanol extracts were suspended in water and extracted successively with hexane, chloroform, and ethyl acetate. The G_2 checkpoint inhibition activity resided in the chloroform-soluble materials that were further fractionated using sequential application of silica gel flash chromatography (eluent, ethyl acetate:methanol, 90:10), Sephadex LH20 chromatography (eluent, methanol), and reversed-phase HPLC[4] (eluent, H_2O:methanol:diisopropylamine, 30:70:0.005). Extracts of *Didemnum granulatum* were fractionated by gel filtration on Sephadex LH-20 (eluent, methanol) followed by reversed-phase HPLC (eluent, acetonitrile:0.05% trifluoroacetic acid, 1:1).

Cytotoxicity Assay. MCF-7 cells and lung adenocarcinoma A549 cells (19), with or without p53 function, were seeded at 800 cells per well in 96-well plates, grown overnight, and irradiated with 0, 2, 4, or 6 Gy. Immediately after irradiation, the cells were treated with different concentrations of isogranulatimide for 16 h. The drug was removed, and cells were allowed to grow in fresh medium until those not treated with isogranulatimide approached confluency, typically between 2 days for unirradiated cells and 4–6 days for cells irradiated with 6 Gy. Cell survival was measured using a soluble tetrazolium salt assay (CellTiter96TM; Promega). One hundred % cell survival was defined as the surviving fraction after irradiation alone. A dose of 6 Gy induced ~80% cell death.

RESULTS AND DISCUSSION

Assay for G_2 Checkpoint Inhibitors. To develop an assay for detecting G_2 checkpoint inhibitors (shown schematically in Fig. 1*A*), we first established a system in which a majority of cells could be reversibly arrested in G_2 by DNA damage. Human breast carcinoma MCF-7 cells, which fail to arrest in G_1 due to the expression of a dominant-negative mutant p53 (MCF-7 mp53; Ref. 18), were subjected to 6.5 Gy of γ-irradiation. About 90% of these cells arrested in G_2-M by 16 h after irradiation, as determined by flow cytometry (Fig. 1, *B–D*). To confirm that the cells were arrested in G_2, the microtubule depolymerizing agent nocodazole was added at the time of irradiation to trap cells in mitosis, and the percentage of mitotic cells was determined at different times using microscopy. No cells entered mitosis between 0 and 20 h, demonstrating complete G_2 arrest during this period (Fig. 1*G*). To demonstrate the reversibility of the G_2 arrest, cells were treated with the G_2 checkpoint inhibitors caffeine or UCN-01 between 16 and 24 h after irradiation. This resulted in release of 50–70% of the cells from G_2 arrest, measured by flow cytometry (Fig. 1, *E* and *F*). We also measured release from G_2 arrest by microscopy, by counting cells accumulating in mitosis in the presence of nocodazole, with similar results (Fig. 1*G*).

We then developed a microtiter plate assay for detecting cells released from G_2 arrest into mitosis in the presence of nocodazole, using an ELISA with monoclonal antibody TG-3. This antibody recognizes a phosphorylated form of nucleolin present during mitosis and stains mitotic cells >50-fold more strongly than interphase cells (29). The relationship between the percentage of mitotic cells measured by microscopy and the signal obtained by ELISA is shown in Fig. 1*H*. The ELISA signal is linear between 0 and 100% mitotic cells,

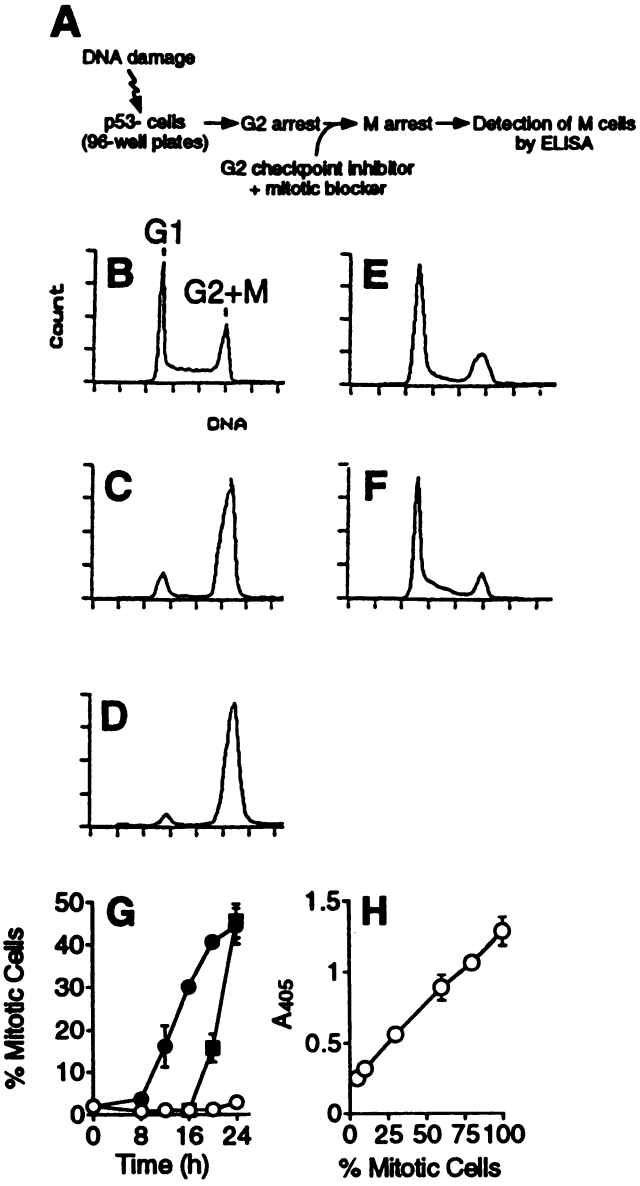

Fig. 1. Development of G_2 checkpoint inhibition assay. *A*, schematic representation of the assay. *B–F*, the cell cycle distribution of MCF-7 mp53 cells after γ-irradiation and exposure to G_2 checkpoint inhibitors was determined by flow cytometry: the *x axis* shows the relative DNA content of the cells determined by intensity of propidium iodide fluorescence, and the *y axis* shows cell number. The G_1 and G_2+M populations are indicated above their respective peaks. Exponentially growing MCF-7 mp53 cells were irradiated with 6.5 Gy and either harvested at 0 (*B*), 16 (*C*) or 24 (*D*) h after irradiation or treated with 2 mM caffeine (*E*) or with 100 nM UCN-01 (*F*) between 16 and 24 h after irradiation. *G*, MCF-7 mp53 cells were irradiated at 0 h with 6.5 Gy, and 0.2 μM nocodazole was added to all samples. The cells were then incubated without caffeine (○), or with 2 mM caffeine added at 0 h (●) or 16 h (■). The percentage of mitotic cells was determined by microscopy at the indicated times. (*H*), the correspondence between ELISA and the percentage of cells in mitosis determined by microscopy for cell populations containing different proportions of mitotic cells. *Data points*, means of triplicate measurements; *bars*, SD.

correlates highly ($r > 0.99$) with the results obtained by microscopy, and has the sensitivity required for use with 96-well plates.

Screen of 1300 Extracts from Marine Organisms. We used this assay to search for G_2 checkpoint inhibitors in extracts from marine invertebrates and their associated microorganisms, which are rich sources of chemically diverse bioactive compounds (30–32). MCF-7 mp53 cells grown in 96-well plates were irradiated to induce G_2 arrest and treated with extracts and nocodazole. Screening of 1300 extracts at two different dilutions yielded 11 samples with significant activity.

[4] The abbreviations used are: HPLC, high-performance liquid chromatography; MS, mass spectrometry; NMR, nuclear magnetic resonance.

A separate screen using VM-26, a topoisomerase II inhibitor which induces DNA strand breaks, as the DNA-damaging agent identified activity in three of these extracts and two additional ones. Here, we report the isolation and identification of two G_2 checkpoint inhibitors.

Identification and Activity of Staurosporine and Two Semisynthetic Analogues. Bacterial isolate Clin-1116 was obtained from the surface of a Northeastern Pacific Ocean sponge. It is an actinomycete by appearance and Gram's stain but has not been identified to a specific genus and species. The active compound was purified from Clin-1116 methanol extracts by chromatographic procedures (see "Materials and Methods") using the G_2 checkpoint inhibition assay to monitor purification. The isolated compound was identified as staurosporine (Fig. 2*A*), one of the few known G_2 checkpoint inhibitors, by analysis of its MS and NMR data and comparison with published values (33, 34). This provided a validation of our assay.

We also isolated two closely related compounds, identified by MS and NMR as the oxazolidine and the carbamate derivatives of staurosporine (Fig. 2). The compounds were not present in the original extract but formed over time when staurosporine was stored in the NMR solvent deuterated chloroform, presumably via reaction with phosgene formed by the decomposition of deuterated chloroform. Reaction of staurosporine with phosgene in dichloromethane generated both the oxazolidine and carbamate derivatives of staurosporine, confirming this hypothesis (see "Appendix").

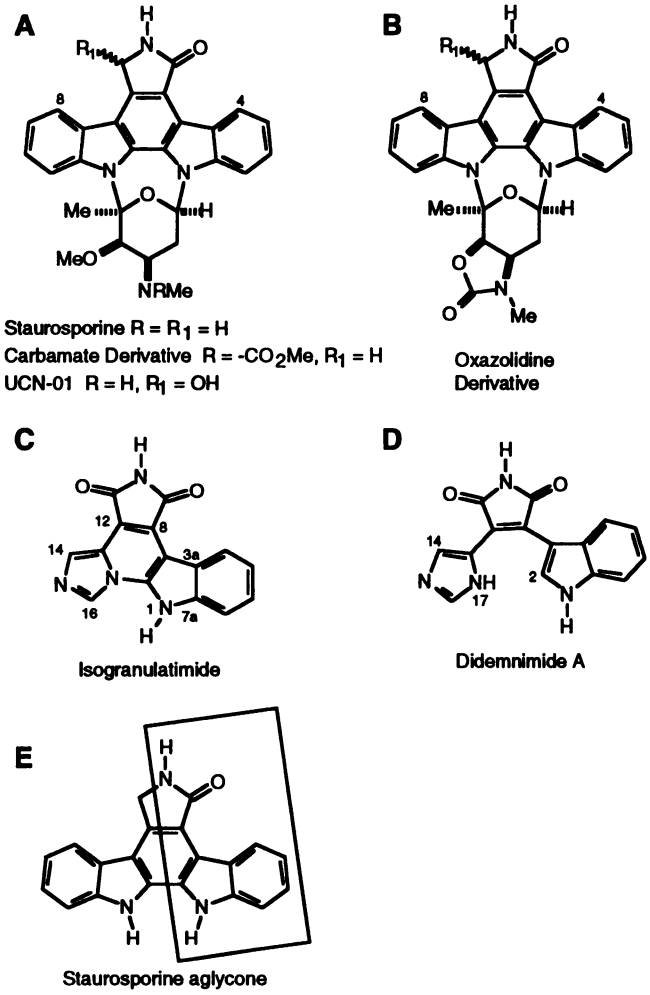

Fig. 2. Chemical structures of staurosporine derivatives, isogranulatimide and didemnimide A. The *box* in *E* shows the region of structural identity between isogranulatimide and staurosporine aglycone.

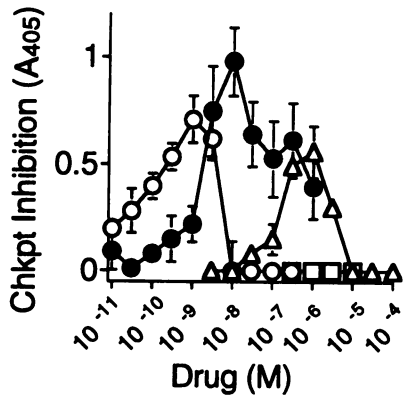

Fig. 3. G_2 checkpoint inhibition by staurosporine and derivatives. G_2 checkpoint inhibition by staurosporine (○), UCN-01 (●), the oxazolidine derivative of staurosporine (△) or the carbamate derivative of staurosporine (□) is expressed as the ELISA signal, in which A_{405} = 1 corresponds to ~60% mitotic cells. *Data points*, means of triplicate measurements; *bars*, SD.

The G_2 checkpoint inhibition and the cytotoxicity of staurosporine and related compounds were also measured. Staurosporine and UCN-01 showed strong G_2 checkpoint inhibition, with IC_{50}s of 0.2 ± 0.2 nM and 6 ± 2 nM, respectively (Fig. 3). The oxazolidine derivative had a higher IC_{50} of 360 ± 20 nM and showed less activity at its optimal concentration (Fig. 3). Interestingly, the carbamate derivative showed no detectable G_2 checkpoint inhibition, even at the highest concentration tested (0.2 mM, Fig. 3), yet retained cytotoxicity (IC_{50} = 14 ± 1 μM). Staurosporine, UCN-01, and the oxazolidine derivative were also significantly cytotoxic when used alone (IC_{50}s of 60 ± 20 nM, 80 ± 10 nM, and 40 ± 10 μM, respectively). UCN-01 did not kill cells synergistically with γ-irradiation in this system (data not shown).

Identification of Isogranulatimide. A second active extract was from the ascidian *D. granulatum* (Subphylum Urochordata, Class Ascidiacea) from Brazil. Fractionation of the extract led to the isolation of the novel compound isogranulatimide (Fig. 2*C*), the known alkaloid didemnimide A (Fig. 2*D*), and several closely related analogues. Didemnimide A was identified by comparison of its NMR and MS data with published values (35).

Isogranulatimide was isolated as a bright orange solid {UV [λ_{max}, nm (ϵ)] 210 (10,200), 231 (10,600), 280 (6,550), 470 (1,870)} that gave a $[M + H]^+$ ion at *m/z* 277.0730 in the high-resolution fast atom bombardment MS appropriate for a molecular formula of $C_{15}H_8N_4O_2$ (calculated mass for $C_{15}H_9N_4O_2$, 277.0714). The molecular formula of isogranulatimide differed from that of didemnimide A only by the loss of two hydrogen atoms, and a comparison of their NMR data (in DMSO-d_6) showed that the two compounds were closely related. An NH proton resonance at δ 11.11 showed heteronuclear multiple bond correlations to carbonyl resonances at δ 169.0 and 170.0 and sp^2 carbon resonances at δ 126.4 and 112.2, confirming the presence of a maleimide substructure in isogranulatimide. The correlation spectroscopy spectrum identified a four proton spin system [δ 8.51, d, J = 6 Hz (H-4)]; 7.43, dd, J = 7,7 Hz (H-6); 7.35, dd, J = 7,7 Hz (H-5); 7.67, d, J = 7 Hz (H-7)) that could be assigned to the H-4 to H-7 protons on an indole residue. Irradiation of a broad proton resonance at δ 13.48 induced a nuclear Overhauser effect only in the aromatic doublet at δ 7.68, which assigned the doublet to H-7 and the broad proton resonance to the indole NH. The absence of a resonance in the ^1H NMR spectrum of isogranulatimide that could be assigned to the indole H-2 proton indicated the presence of a substituent at C-2. Subtraction of the atoms present in the maleimide and indole fragments ($C_{12}H_6N_2O_2$) from the molecular formula of isogranulatimide

left $C_3H_2N_2$. These atoms could be accounted for by a disubstituted imidazole moiety leading to the conclusion that isogranulatimide was a cyclized analogue of didemnimide A with a bond between C-2 of the indole and either C-14 or N-17 of the imidazole ring. The large chemical shift observed for the H-4 resonance (δ 8.51) in isogranulatimide relative to the chemical shift observed for the H-4 resonance in didemnimide A (δ 7.07) was attributed to a neighboring group effect from the C-9 maleimide carbonyl in isogranulatimide. A similar anisotropic effect deshields the H-4 resonance (DMSO-d_6 δ 9.30) relative to the H-8 resonance (δ 7.96) in staurosporine (34). The presence of the anisotropic effect in isogranulatimide and not in didemnimide A provides strong support for the proposal that isogranulatimide is a rigid planar heterocycle, unlike didemnimide A, in which the indole and maleimide rings are twisted relative to each other along the C-3—C-8 bond (35). Two remaining resonances at δ 8.10 and 9.12 in the ^{1}H NMR spectrum, which could be assigned to the imidazole fragment of isogranulatimide, gave very broad signals that failed to show any heteronuclear multiple bond/heteronuclear multiple quantum correlations or nuclear Overhauser effects, precluding a clear spectroscopic resolution to the structural problem. Therefore, to determine whether isogranulatimide had a C-2—C-14 or C-2—N-17 bond, both isomers were prepared by unambiguous total synthesis.[5] Comparison of the NMR and UV data obtained for the natural product with the data obtained for the authentic synthetic materials revealed that isogranulatimide was the isomer with the C-2—N-17 bond, as shown in Fig. 2*C*. The heterocyclic aromatic core of isogranulatimide appears to be without precedent in natural products.

Isogranulatimide Selectively Potentiates the Killing of p53 Cells by γ-Irradiation. Isogranulatimide showed half-maximal G_2 checkpoint inhibition at 1.8 ± 0.2 μM (Fig. 4*A*). Didemnimide A showed no activity at all concentrations tested (0.1–30 μM; data not shown). Isogranulatimide alone showed mild cytotoxicity to MCF-7 cells with or without p53 function (IC_{50} = 40 ± 4 μM; Fig. 4, *B* and *C*; curve = 0 Gy), well above the IC_{50} for checkpoint inhibition. When MCF-7 cells with wild-type p53 function were exposed to 2, 4, or 6 Gy of γ-irradiation and to different concentrations of isogranulatimide for 16 h, the level of cell death was the same as or lower than the sum of either treatment alone (Fig. 4*B*). However, when MCF-7 mp53 cells were treated in the same way (Fig. 4*C*), cells died in much higher numbers than the sum of either treatment alone, showing that isogranulatimide acts synergistically with radiation in cells lacking p53 function. Isogranulatimide alone showed very little cytotoxicity toward lung adenocarcinoma A549 cells (8) with wild-type p53 (IC_{50} > 100 μM) but was significantly more toxic to A549 cells lacking p53 function (IC_{50} = 37 μM). As shown for MCF-7 cells, γ-irradiation and isogranulatimide killed A549 cells without p53 function synergistically (Fig. 4*D*) but not A549 cells with wild-type p53.

Structural Similarities between Isogranulatimide, Staurosporine, and Didemnimide A. Isogranulatimide shows some resemblance to staurosporine (Fig. 2). It is identical to staurosporine aglycone over the boxed region in Fig. 2*E* except for the presence of a carbonyl group at position 11, an indole group instead of an imidazole, and a N instead of a C at position 17. The staurosporine aglycone shows no G_2 checkpoint inhibition over a wide concentration range (data not shown), implying that the region found only in isogranulatimide is important for G_2 checkpoint inhibition. Staurosporine and UCN-01 differ only by the presence of a hydroxyl group at R1 (Fig. 2*A*), yet UCN-01 consistently shows more activity at its optimal concentration than staurosporine, indicating that this modification contributes to G_2 checkpoint inhibition. Isogranulatimide has a carbonyl at the corresponding position, which may also play a role. In addition, the carbamate derivative of staurosporine, which bears a modified sugar, showed no G_2 checkpoint inhibition, indicating that the sugar portion is critically important for staurosporine's activity. These results indicate that, despite a degree of structural similarity, isogranulatimide and staurosporine may act on different cellular targets.

Isogranulatimide and didemnimide A differ only by the presence of a bond between C-2 and N-17 (Fig. 2, *C* and *D*), yet didemnimide A is inactive as a checkpoint inhibitor. The indole, maleimide, and imidazole moieties of didemnimide A are twisted with respect to each other along the C-3—C-8 and the C-12—C-13 bonds (35). The C-2—N-17 bond makes isogranulatimide a rigid planar heterocycle, a structural feature found in some protein kinase inhibitors (36), suggesting that isogranulatimide inhibits the activity of a protein kinase

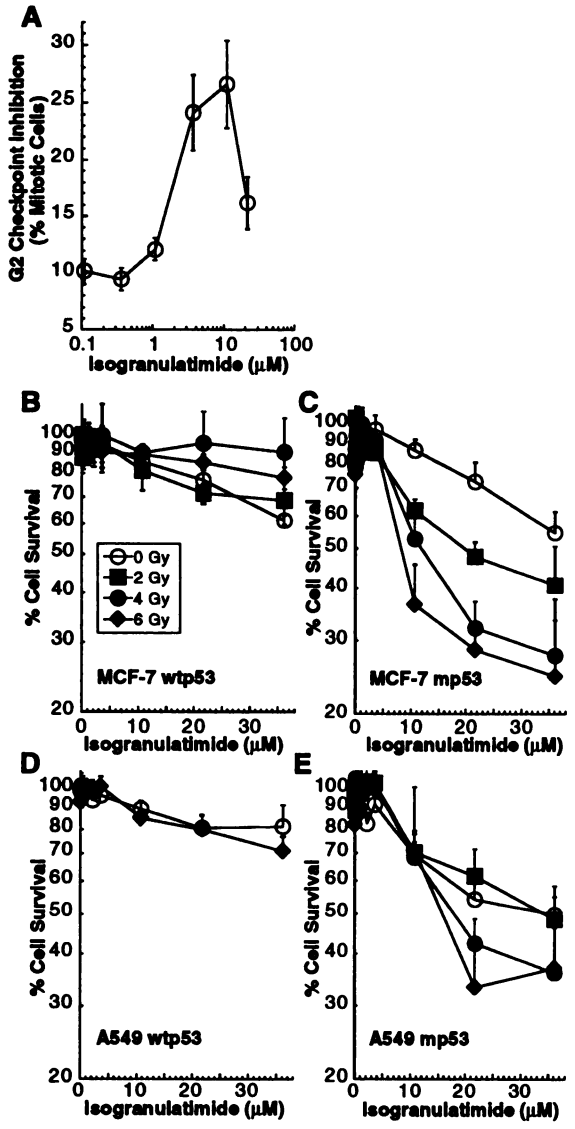

Fig. 4. Activity of isogranulatimide. *A*, G_2 checkpoint inhibition. *B–E*, cytotoxicity of isogranulatimide in combination with γ-irradiation to MCF-7 cells (*B* and *C*) and A549 cells (*D* and *E*) with wild-type p53 (p53+) or loss of p53 function (p53−). *Data points*, means of triplicate measurements; *bars*, SD.

[5] R. G. S. Berlinck, R. Britton, E. Piers, L. Lim, M. Roberge, R. Moreira da Rocha, and R. J. Andersen, Granulatimide and isogranulatimide, aromatic alkaloids with G_2 checkpoint inhibition activity isolated from the Brazilian ascidian *Didemnum granulatum*: structure elucidation and synthesis. J. Org. Chem., in press.

that is required for G_2 arrest. Isogranulatimide, staurosporine, the oxazolidine derivative of staurosporine, and UCN-01 all showed a decline in activity at high concentrations (Figs. 3 and 4). This probably reflects the inhibition of additional kinases that are required for mitotic entry, such as cyclin-dependent kinases (26, 37), and not a loss of activity at high concentrations.

Perspectives. According to a recent speculative model of the G_2 checkpoint, the transduction of a signal generated by DNA damage requires the activity of the ATM, ATR, and Chk1 protein Ser/Thr kinases and of the Wee1 or Myt1 protein Tyr kinase (38). We hypothesize that isogranulatimide inhibits one or more of these kinases. If this is not the case, identification of isogranulatimide's target may provide important new information about the biochemical mechanism of the G_2 checkpoint.

Isogranulatimide selectively enhances γ-irradiation-induced killing in MCF-7 cells lacking p53 function while showing low cytotoxicity alone, warranting its consideration as a lead compound for experimental cancer therapy. Our current efforts at purifying and identifying inhibitors from this original screen of 1300 extracts have yielded at least one additional new class of compounds. The availability of a reliable assay for drug screening and of candidate drugs will help test and develop this therapeutic strategy.

ACKNOWLEDGMENTS

We thank R. Moreira da Rocha (Universidade Federal do Parana) for collection and identification of the ascidian *Didemnum granulatum*.

APPENDIX

While collecting ^{1}H NMR data on a sample of staurosporine dissolved in $CDCl_3$, we observed the appearance of new minor signals in the spectrum over time. Analysis of this sample revealed the presence of a compound that was not present originally. This compound was isolated by reversed-phase HPLC (eluent, H_2O:methanol: diisopropylamine, 30:70:0.005) and shown by MS and NMR analysis to be the oxazolidine derivative of staurosporine. Spectroscopic data were as follows: HREIMS *m/z* 478.1641 ($C_{28}H_{22}N_4O_4$; requires 478.1636); ^{1}H NMR (DMSO-d_6) δ 7.78, d, J = 8.2 Hz (H1), 7.52, dd, J = 7.6, 8.2 Hz (H2), 7.30, dd, J = 7.6, 7.9 Hz (H3), 9.22, d J = 7.9 Hz (H4), 8.63, s (H6), 4.98, d, J = 6.3 Hz (H7), 8.03, d, J = 7.6 Hz (H8), 7.38, dd, J = 7.6, 7.6 Hz (H9), 7.51, dd, J = 7.6, 8.4 Hz (H10), 8.06, d, J = 8.4 Hz (H11), 5.31, d, J = 8.7 Hz (H3'), 4.34, m (H4'), 1.97, m (H5'α), 2.91, m (H5'β), 6.96, dd, J = 6.4, 9.8 Hz (H6'), 2.03, s (2'Me), 2.58, s (N-Me); ^{13}C NMR (DMSO-d_6) 108.6 (C1), 125.4 (C2), 119.5 (C3), 125.4 (C4), 122.3 (C4a), 115.4 (C4b), 132.9 (C4c), 171.5 (C5), 45.2 (C7), 120.3 (C7a), 115.6 (C7b), 124.9 (C7c), 121.2 (C8), 120.9 (C9), 124.6 (C10), 116.6 (C11), 140.3 (C11a), 125.7 (C12a), 128.6 (C12b), 136.4 (C13a), 92.5 (C2'), 75.4 (C3'), 52.0 (C4'), 45.2 (C5'), 79.1 (C6'), 155.6 (C7'), 28.7 (NMe), 29.5 (2'Me). It appeared likely that the $CDCl_3$ used in the NMR experiment had partially decomposed to generate phosgene, which in turn had reacted with staurosporine to give the new derivative. To confirm this supposition, pure staurosporine (50 mg) was dissolved in a mixed solvent of $CHCl_3$ (20 ml) and methanol (5 ml), and phosgene gas was bubbled through the solution for 2 min. The reaction mixture was purified using silica gel flash chromatography (eluent, EtOAc:methanol, 90: 10) and reversed-phase HPLC (eluent 1, methanol:H_2O, 7:3; eluent 2, methanol:H_2O:diisopropylamine, 55:45:0.005) to give pure oxazolidine (40% yield), carbamate (6% yield), and aglycone (12% yield) derivatives (39) and unreacted staurosporine. The structures of the new carbamate and the known aglycone were identified by analysis of their MS and NMR data and in the case of the aglycone, comparison with literature values. Spectroscopic data for the carbamate derivative were: HRFABMS *m/z* 525.2124 [$C_{30}H_{28}N_4O_5$ (M + H), requires 525.2124]; ^{1}H (DMSO-d_6) δ 7.64, d, J = 8.2 Hz (H1), 7.48, dd, J = 7.5, 8.2 Hz (H2), 7.29, dd, J = 7.5, 8.0 Hz (H3), 9.27, d, J = 8.0 Hz (H4), 8.55, s (H6), 4.98, s (H7), 8.05, d, J = 7.6 Hz (H8), 7.35, dd, J = 7.5, 7.6 Hz (H9), 7.49, dd, J = 7.5, 8.4 Hz (H10), 8.00, d, J = 8.4 Hz (H11), 4.28, s (H3'), 4.65, bm (H4'), 2.25, m (H5'α), 2.63, m (H5'β), 7.01 bm (H6'), 2.35, s (2'Me), 2.69, s (N-Me), 2.69, s (3'OMe), 3.71, s (CO_2Me); ^{13}C (DMSO-d_6) 108.2(C1), 124.6 (C2), 118.9 (C3), 125.7 (C4), 122.5 (C4a), 113.5 (C4b), 118.8 (C4c), 171.9 (C5), 45.4 (C7), 119.4 (C7a), 114.1 (C7b), 123.8 (C7c), 121.5 (C8), 120.4 (C9), 125.0 (C10), 113.5 (C11), 138.7 (C11a), 129.2 (C12a), 125.4 (C12b), 136.2 (C13a), 94.6 (C2'), 83.8 (C3'), 50.3 (C4'), 29.1 (C5'), 82.2 (C6'), 156.8 (C7'), 29.9 (NMe), 29.1 (2'Me), 60.3 (3'OMe), 52.8 (CO_2Me). Reaction of staurosporine with phosgene to give the oxazolidine derivative represents a new type of transformation of the staurosporine structure to give a bioactive derivative.

REFERENCES

1. Hartwell, L., Weinert, T., Kadyk, L., and Garvik, B. Cell cycle checkpoints, genomic integrity, and cancer. Cold Spring Harbor Symp. Quant. Biol., *59:* 259–263, 1994.
2. Kaufmann, W. K., and Paules, R. S. DNA damage and cell cycle checkpoints. FASEB J., *10:* 238–247, 1996.
3. Kastan, M. B., Onyekwere, O., Sidransky, D., Vogelstein, B., and Craig, R. W. Participation of p53 protein in the cellular responses to DNA damage. Cancer Res., *51:* 6304–6311, 1991.
4. Paules, R. S., Levedakou, E. N., Wilson, S. J., Innes, C. L., Rhodes, N., Tlsty, T. D., Galloway, D. A., Donehower, L. A., Tainsky, M. A., and Kaufmann, W. K. Defective G_2 checkpoint function in cells from individuals with familial cancer syndromes. Cancer Res., *55:* 1763–1773, 1995.
5. Murray, A. W. Creative blocks: cell-cycle checkpoints and feedback controls. Nature (Lond.), *359:* 599–604, 1992.
6. Weinert, T., and Lydall, D. Cell cycle checkpoints, genetic instability and cancer. Semin. Cancer Biol., *4:* 129–140, 1993.
7. Nurse, P. Checkpoint pathways come of age. Cell, *91:* 865–867, 1997.
8. Kao, G. D., McKenna, W. G., Maity, A., Blank, K., and Muschel, R. J. Cyclin B1 availability is a rate-limiting component of the radiation-induced G_2 delay in HeLa cells. Cancer Res., *57:* 753–758, 1997.
9. Busse, P. M., Bose, S. K., Jones, R. W., and Tolmach, L. J. The action of caffeine on X-irradiated HeLa cells III. Enhancement of X-ray-induced killing during G_2 arrest. Radiat. Res., *76:* 292–307, 1978.
10. Schlegel, R., and Pardee, A. B. Caffeine-induced uncoupling of mitosis from the completion of DNA replication in mammalian cells. Science (Washington DC), *232:* 1264–1266, 1986.
11. Downes, C. S., Musk, S. R. R., Watson, J. V., and Johnson, R. T. Caffeine overcomes a restriction point associated with DNA replication, but does not accelerate mitosis. J. Cell Biol., *110:* 1855–1859, 1990.
12. Steinmann, K. E., Belinski, G. S., Lee, D., and Schlegel, R. Chemically induced premature mitosis: differential response in rodent and human cells and the relationship to cyclin B synthesis and $p34^{cdc2}$/cyclin B complex formation. Proc. Natl. Acad. Sci. USA, *88:* 6843–6847, 1991.
13. Andreassen, P. R., and Margolis, R. L. 2-Aminopurine overrides multiple cell cycle checkpoints in BHK cells. Proc. Natl. Acad. Sci. USA, *89:* 2272–2276, 1992.
14. Tam, S. W., and Schlegel, R. Staurosporine overrides checkpoints for mitotic onset in BHK cells. Cell Growth Differ., *3:* 811–817, 1992.
15. Wang, Q., Fan, S., Eastman, A., Worland, P. J., Sausville, E. A., and O'Connor, P. M. UCN-01: a potent abrogator of G_2 checkpoint function in cancer cells with disrupted p53. J. Natl. Cancer Inst. (Bethesda), *88:* 956–965, 1996.
16. Roberge, M., Tudan, C., Hung, S. M., Harder, K. W., Jirik, F. R., and Anderson, H. Antitumor drug fostriecin inhibits the mitotic entry checkpoint and protein phosphatases 1 and 2A. Cancer Res., *54:* 6115–6121, 1994.
17. Yamashita, K., Yasuda, H., Pines, J., Yasumoto, K., Nishitani, H., Ohtsubo, M., Hunter, T., Sugimura, T., and Nishimoto, T. Okadaic acid, a potent inhibitor of type 1 and type 2A protein phosphatases, activates Cdc2/H1 kinase and transiently induces a premature mitosis-like state in BHK21 cells. EMBO J., *9:* 4331–4338, 1990.
18. Fan, S., Smith, M. L., Rivet, D. J., II, Duba, D., Zhan, Q., Kohn, K. W., Fornace, J. A., Jr., and O'Connor, P. M. Disruption of p53 function sensitizes breast cancer MCF-7 cells to cisplatin and pentoxifylline. Cancer Res., *55:* 1649–1654, 1995.
19. Russell, K. J., Wiens, L. W., Demers, G. W., Galloway, D. A., Plon, S. E., and Groudine, M. Abrogation of the G_2 checkpoint results in differential radiosensitization of G1 checkpoint-deficient and G1 checkpoint-competent cells. Cancer Res., *55:* 1639–1642, 1995.
20. Powell, S. N., DeFrank, J. S., Connell, P., Eogan, M., Preffer, F., Dombkowski, D., Tang, W., and Friend, S. Differential sensitivity of p53- and p53+ cells to caffeine-induced radiosensitization and override of G_2 delay. Cancer Res., *55:* 1643–1648, 1995.
21. Russell, K. J., Wiens, L. W., Demers, G. W., Galloway, D. A., Le, T., Rice, G. C., Bianco, J. A., Singer, J. W., and Groudine, M. Preferential radiosensitization of G1

checkpoint-deficient cells by methylxanthines. Int. J. Radiat. Oncol. Biol. Phys., *36:* 1099–1106, 1996.

22. Yao, S-L., Akhtar, A. J., McKenna, K. A., Bedi, G. C., Sidransky, D., Mabry, M., Ravi, S. J., Collector, M. I., Jones, R. J., Sharkis, S. J., Fuchs, E. J., and Bedi, A. Selective radiosensitization of p53-deficient cells by caffeine-mediated activation of $p34^{cdc2}$ kinase. Nat. Med., *2:* 1140–1143, 1996.
23. Bracey, T. S., Williams, A. C., and Paraskeva, C. Inhibition of radiation-induced G_2 delay potentiates cell death by apoptosis and/or the induction of giant cells in colorectal tumor cells with disrupted p53 function. Clin. Cancer Res., *3:* 1371–1381, 1997.
24. Bunch, R. T., and Eastman, A. Enhancement of cisplatin-induced cytotoxicity by 7-hydroxystaurosporine (UCN-01), a new G_2-checkpoint inhibitor. Clin. Cancer Res., *2:* 791–797, 1996.
25. Mizuno, K., Noda, K., Ueda, Y., Hanaki, H., Saido, T. C., Ikuta, T., Kuroki, T., Tamaoki, T., Hirai, S., Osada, S., and Ohno, S. UCN-01, an anti-tumor drug, is a selective inhibitor of the conventional PKC subfamily. FEBS Lett., *359:* 259–261, 1995.
26. Kawakami, K., Futami, H., Takahara, J., and Yamaguchi, K. UCN-01, 7-hydroxylstaurosporine, inhibits kinase activity of cyclin-dependent kinases and reduces the phosphorylation of the retinoblastoma susceptibility gene product in A459 human lung cancer cell line. Biochem. Biophys. Res. Commun., *219:* 778–783, 1996.
27. Anderson, H. J., Coleman, J. E., Andersen, R. J., and Roberge, M. Cytotoxic peptides hemiasterlin, hemiasterlin A and hemiasterlin B induce mitotic arrest and abnormal spindle formation. Cancer Chemother. Pharmacol., *39:* 223–226, 1997.
28. Vincent, I., Rosado, M., and Davies, P. Mitotic mechanisms in Alzheimer's disease? J. Cell Biol., *132:* 413–425, 1996.
29. Anderson, H. J., deJong, G., Vincent, I., and Roberge, M. Flow cytometry of mitotic cells. Exp. Cell Res., *238:* 498–502, 1998.
30. Attaway, D., and Zaborsky, O. (eds.). Marine Biotechnology: Pharmaceutical and Bioactive Natural Products, Vol. 1. New York: Plenum Press, 1993.
31. Fautin, D. G. (ed.). Biomedical Importance of Marine Organisms. San Francisco: California Academy of Sciences, 1988.
32. Faulkner, D. J. Chemical riches from the oceans. Chem. Br., *31:* 681–684, 1995.
33. Omura, S., Iwai, Y., Hirano, A., Nakagawa, A., Awaya, J., Tsuchya, H., Takahashi, Y., and Masuma, R. A new alkaloid AM-2282 of *Streptomyces* origin. Taxonomy, fermentation, isolation and preliminary characterization. J. Antibiot. (Tokyo), *30:* 275–282, 1977.
34. Takahashi, I., Saitoh, Y., Yoshida, M., Sano, H., Nakano, H., Morimoto, M., and Tamaoki, T. UCN-01 and UCN-02, new selective inhibitors of protein kinase C. II. Purification, physico-chemical properties, structural determination and biological activities. J. Antibiot. (Tokyo), *42:* 571–576, 1989.
35. Vervoort, H. C., Richards-Gross, S. E., Fenical, W., Lee, A. Y., and Clardy, J. Didemnimides A–D. Novel, predator-deterrent alkaloids from the Caribbean mangrove ascidian *Didemnum conchyliatum*. J. Org. Chem., *62:* 1486–1490, 1997.
36. Hidaka, H., and Kobayashi, R. Pharmacology of protein kinase inhibitors. Annu. Rev. Pharmacol. Toxicol., *32:* 377–387, 1992.
37. Guo, X. W., Th'ng, J. P., Swank, R. A., Anderson, H. J., Tudan, C., Bradbury, E. M., and Roberge, M. Chromosome condensation induced by fostriecin does not require $p34^{cdc2}$ kinase activity and histone H1 hyperphosphorylation, but is associated with enhanced histone H2A and H3 phosphorylation. EMBO J., *14:* 976–985, 1995.
38. Weinert, T. A DNA damage checkpoint meets the cell cycle engine. Science (Washington DC), *277:* 1450–1451, 1997.
39. Yasuzawa, T., Iida, T., Yoshida, M., Hirayama, N., Takahashi, M., Shirahata, K., and Sano, H. The structures of the novel protein kinase inhibitors K-252a, b, c, and d. J. Antibiot. (Tokyo), *39:* 1072–1078, 1986.